Venkatesh et al. 2018. *Int. J. Vehicle Structures & Systems*, 10(4), 226-230
ISSN: 0975-3060 (Print), 0975-3540 (Online)
doi: 10.4273/ijvss.10.4.01

International Journal of Vehicle Structures & Systems
Available online at www.maftree.org/eja

Effects of Delamination on the Critical Buckling Load of Glass Fiber Reinforced Epoxy Composite Plates

S. Venkatesh[a], S. Prakash, S. Raja, S. Manigandan and P. Sivashankari

School of Mech. Engg., Sathyabama Inst. of Sci. and Tech., Chennai, India
[a]Corresponding Author, Email: mitvenkatesh@gmail.com

ABSTRACT:

The effects of the delamination in the critical buckling load failure of E-Glass /epoxy composite laminates are analysed. The buckling load of rectangular composite plates is determined by carrying out the experimental work for different aspect ratios of range 2 to 3. The specimens are made with unidirectional fibres of orientation (90 °/45 °/-45 °/0 °)s. The width of long 100 mm and 50 mm at the centre of the plate, a single substantial delamination is made at the mid layer produced by Teflon film using hand lay-up technique. The buckling loads of plates were found by using simply supported boundary condition and kept the other side edges free. The experimental buckling loads were found from the graph drawn for vertical displacement vs load. By drawing the graph for the vertical displacement vs. load, the experimental buckling load can be calculated. Using finite element software of ANSYS 10, the experimental results were validated.

KEYWORDS:

Epoxy composites; Glass fibre; Buckling; Reinforcement; Delamination; Mechanical properties

CITATION:

S. Venkatesh, S. Prakash, S. Raja, S. Manigandan and P. Sivashankari. 2018. Effects of Delamination on the Critical Buckling Load of Glass Fiber Reinforced Epoxy Composite Plates, *Int. J. Vehicle Structures & Systems*, 10(4), 226-230. doi:10.4273/ijvss.10.4.01.

1. Introduction

Most of the research is carried out to enhance the mechanical properties of the composite materials and its recyclability by applying new materials [1]. Moreover, the manufacturing method is improved by a combination of new materials [2]. Though this has affirmative effects on both the fuel consumption of vehicles and on the cost of the transportation but due to critical fracture load, slender structures can easily get failed [3]. Because of the limited data on the failure behaviour of composite laminates in primary structural components with reliability and integrity, their application also restricted to secondary structures [4]. From a thick layer of the lamina, Fibre reinforced composite materials for structural applications are made. By stacking the layers to achieve desired strength and stiffness, the structural elements such as bars, beams and plates are formed [5], [6]. With the recent development of the fibre reinforced composites, its application has been increasing in numbers [7-8]. There is a critical requirement of a better understanding of material damage tolerance, structural stability, and failure is needed.

The important part of the design process is an estimation of the critical buckling load for different load cases [9-10]. The most common failure modes of composite laminates is the delamination , which usually occurs with the outcome of imperfections in the production process for the effects of external factors, such as impact by forging objects during operation of the composite laminates and the high inter-laminar stress at the free edge impact and fabrication defects[12], [5]. The overall stiffness of the material can be reduced by the presence of delamination, and it results in material unbalancing in the symmetric laminate, as well as the stress within the composite laminate, will be redistributed. This leads to global structural failure below the design level, which reduces the buckling load of the laminate [9]. Besides, the cost of fibre reinforced composites is susceptible to delamination [11]. The Kevlar or Twaron stitched glass/epoxy composite laminates with delamination of different length on the buckling load to obtain critical delamination length [13].

The glass/epoxy composites laminate has the better damage tolerance after it has first buckled as compared to an unstitched or Twaron stitched glass/epoxy composite laminates [14]. Pan [15] determined the effect of the stitching parameter in buckling of plates is determined by using the energy method and investigated stitching density, thread diameter and Young's modulus of the stitching thread [7] [16]. Through thickness, stitching is a promising method to increase the resistance to delamination extension. This increased resistance to delamination is attributed to the increase in the local buckling strength. Kardomateas used the thin film approach to determine the analytical solutions for beams and plates [8], [17]. One dimensional analysis was carried out for both analytically and numerically for single and multiple delaminations [18]. Using the thin film approach analytical solutions was carried out for beams and plates by Chai [8], [17]. Lim gave a solution based on the energy method for multiple delaminated

beams like specimens. Based on the classical beam theory, Shu gave an analytical solution for double delamination buckling. Rodman incorporated the shearing effect by Reissner's beam theory [19-21].

Kim and Kedward solved two-dimensional plate models analytically in the simply supported case using the Navier solution [22-24]. The reduced stiffness zone for plates through the width delamination is determined, when two edges are simply supported and the other ends have arbitrary boundary conditions. The analytical solution used numerical techniques for analysing composite specimens. Kharazi and Ovesy used the Rayleigh-Ritz method to solve the width delaminated composite laminates subjected to compressive loads by the classical laminated plate theory [25]. The semi-analytical methods for different buckling phenomena such as for dynamic buckling were developed then. Ovesy developed the finite strip method based on the analytical integration of energy and work [10]. Zuleyha carried out the investigation on the effect of the delamination size on the compressive failure load and critical buckling load of E-glass / epoxy composite laminates with multiple large delamination induced by low-velocity impact [26]. Most of the stability studies regarding composite plates stacking sequence have paid attention to rectangular plates under simply supported conditions to minimize the mathematical complexities. Hence we have to give more importance to its structural behaviour, the interaction among stacking sequence and length / width ratio on the buckling behaviour of woven fibre laminated composites are needed to investigate.

This work aims at predicting the failure behaviour of composite material for with delamination and without delamination. This project includes the study of buckling analysis of composite plates with different aspect ratio. The lay-up sequence of unidirectional reinforced "plies" and they are typically a thin (approximately 0.2 mm) sheet of collimated fibres impregnated with an uncured epoxy or other thermosetting polymer matrix material. The orientation of each ply is arbitrary, and the layup sequence is tailored to achieve the properties desired of the laminate. The composites are subjected to axial compression, and buckling analysis performed both experimentally and numerically.

2. Fabrications of composites

The industry has evolved over a dozen separate manufacturing processes as well as some hybrid processes to meet the wide range of needs in fabricating the composite. Each of these processes offers advantages and specific benefits which may apply to the fabricating of composites. Hand lay-up and spray-up are two fundamental moulding processes. The hand lay-up process is the oldest, simplest, and most labour intense fabrication method. The process is most common in FRP marine construction. In hand lay-up method, the liquid resin is placed along with reinforcement (woven glass fibre) against the completed surface of the mould. The reaction takes place in the resin that hardens the material to a lightweight and much stronger product. The laminated composite plates with delamination and without delamination are fabricated with (90°/45°/-45°/0°)s fibre orientation from the unidirectional E-Glass fibre and epoxy resin. For matrix materials, epoxy CY-558 and anhydride HY-225 are mixed in the mass ratio of 100:80. Unidirectional E-Glass/epoxy composite plate (Fig. 1) is produced by using hand lay-up technique. The fibre volume fraction is approximately 65%. Each case contains three specimens. The delamination is introduced by inserting 100 μm nylon film during the stacking sequence. This delamination is introduced to simulate the damage induced by the low-velocity impact.

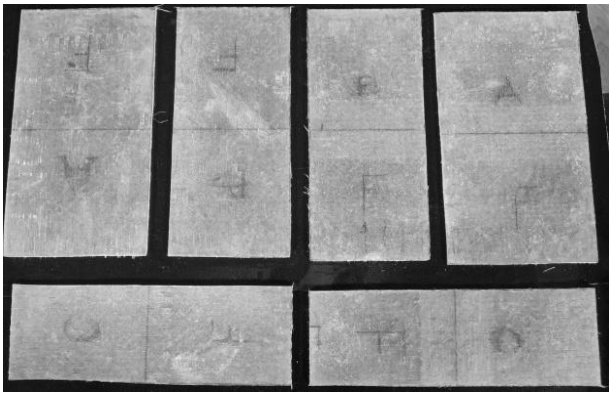

Fig. 1: Fabricated composite plate(s)

3. Experimental buckling analysis

The composite plates support greater compressive load beyond the buckling load, and the numerical studies are performed on the buckling behaviour of the plate. The buckling behaviour is given more importance than the post-buckling behaviour of the composite plates, which carries the additional load before the ultimate load is reached. The abrupt deformation occurs when the stored membrane energy is converted into ending energy with no change in the externally applied load. The total stiffness becomes singular during the buckling is $(k - \lambda kg)\ d = 0$, Where Kg is the geometric stiffness matrix, and it is independent of the material properties of the structure in contrast to the conventional structural stiffness matrix. The multiplier λ represents the factor to the applied load to cause buckling and the computation of buckling load factors is analysed through the modal analysis. The linear buckling is determined by the buckling loads and the associated mode shapes of Eigenvalue buckling problems. The quantities to be computed include the critical loads at which the structure becomes unstable, and the corresponding buckling load shapes in the buckling analysis.

The properties of E-glass/epoxy composites are Major Young's modulus E_L = 537.79 N/mm^2, Minor young's modulus E_T = 179.263 N/mm^2, Major Poisson's ratio μ_{LT} = 0.25, Shear modulus G_{LT} = 89.63 N/mm^2. The test specimen used for buckling load test has dimensions of 100mm, 80mm, and 66mm width, 200mm length and contain 8 plies, with (90°/45°/-45°/0°)s ply orientation. The buckling load test setup contains specially designed jaws that impart simply supported loading edge (SSE) condition. The crosshead speed was kept 0.5mm/min during the test. The specimen was loaded in axial compression using a uniaxial tensile testing machine of 100-tonne capacity. The specimen was clamped at other two ends and kept free at the other

two ends as shown in Fig. 2. A dial gauge was placed at the centre of the specimen to observe the lateral deflection and all the specimens were loaded slowly up to failure. Clamped boundary conditions were stimulated along the top and bottom edges, restraining 40 mm length. For axial loading, the test specimen was placed between the two extreme stiff machine heads, of which the lower one was fixed during the test, whereas the upper head was moved downwards by the servo-hydraulic cylinder.

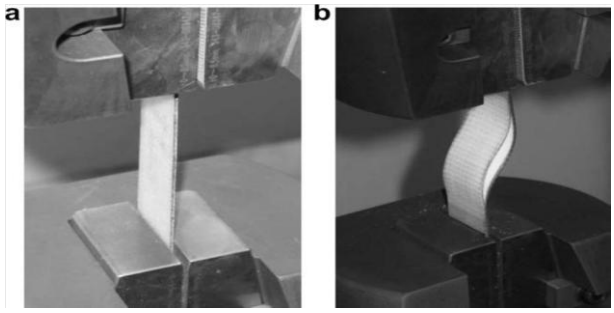

Fig. 2: Buckling test - (a) Before test, (b) Post-test for specimen with delamination

All laminated plates were loaded at the constant cross-head speed of 1 mm/min (200 kN load cell). From Instron 3669 testing machine, while conducting the experiments, a plot between the applied compressive loads against the specimen's axial displacements are obtained. The buckling load is obtained by taking the compressive load at the intersection of the first two tangents drawn from the pre-buckling and post-buckling regions. Figs. 3(a-c) and Figs. 4(a-c) show the vertical load vs. displacement plots for no delamination and with delamination glass/proxy composite laminates of specimen A, B, C having a delamination of 50 mm. The comparisons of experimental buckling loads of composite plates with delamination and without delamination are given in Table 1. The experimental buckling loads of composite plates with delamination were lesser than those without delamination as expected.

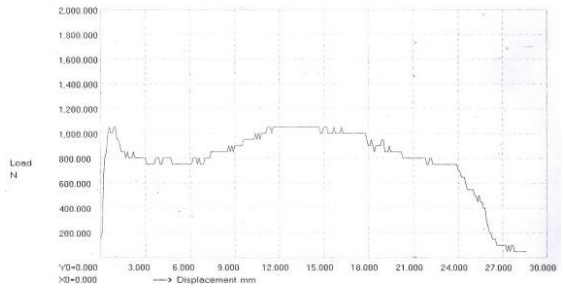

Fig. 3(a): Specimen A without delamination

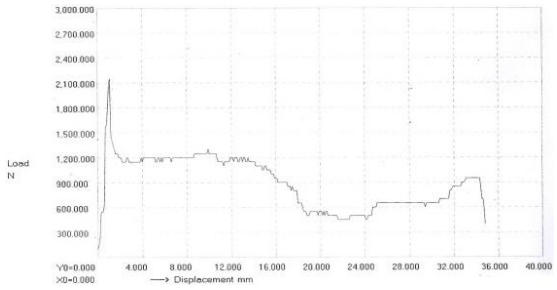

Fig. 3(b): Specimen B without delamination

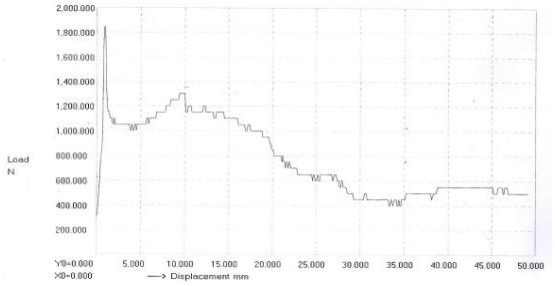

Fig. 3(c): Specimen C without delamination

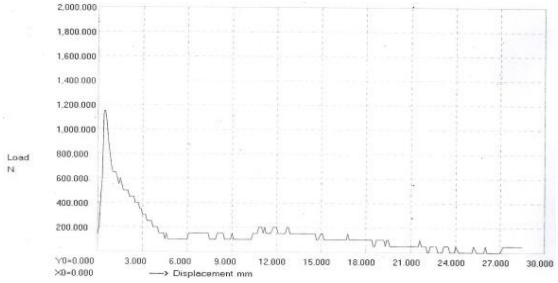

Fig. 4(a): Specimen A with delamination

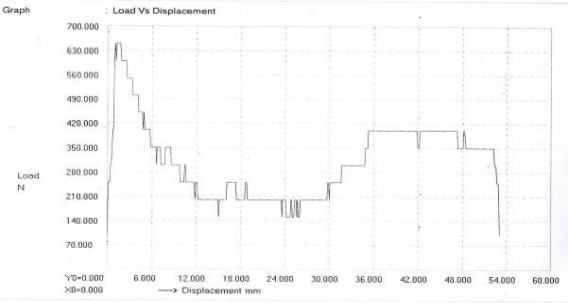

Fig. 4(b): Specimen B with delamination

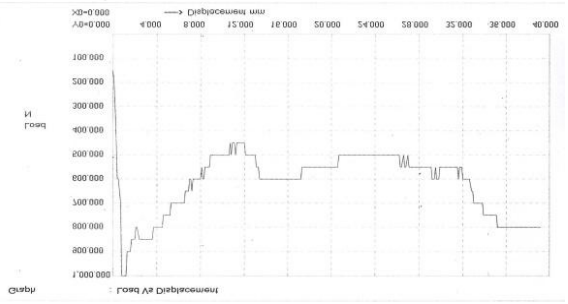

Fig. 4(c): Specimen C with delamination

Table 1: Critical buckling loads from experiments

Specimen name	Specimen size, mm	Experimental buckling load, N	
		No delamination	With delamination
A	200×100	1050	1150
B	200×80	2150	650
C	200×66	1850	1000

4. Finite element modelling and analysis

The finite element method is used for validating the experimental result of the buckling load. Using ANSYS, buckling analysis can be carried out by Eigenvalues approach. SOLID46 layered elements with six degrees of freedom are chosen for meshing the plates. The simply supported loaded edges are simulated with the displacements UX, UY, UZ and the rotations, ROTY, ROTZ of all nodes at the edges are set equal to zero. Then the linear buckling analysis is carried out for the

meshed models with and without delamination. The first buckling mode shapes for all the specimens are presented in Figs. 5(a-c) and Figs. 6(a-c). A comparison of numerical buckling loads of composite plates with and without delamination is given in Table 2. The numerical buckling loads of composite plates with delamination have lesser value than those without delamination. The comparisons of experimental buckling loads of composite plates with delamination without delamination with numerical analysis are presented in Table 3. This difference in the value of buckling loads from numerical analysis is in good agreement with the buckling tests of the composite plate with delamination and without delamination.

Table 2: Summary of numerical buckling load

Specimen name	Specimen size, mm	Numerical buckling load, N	
		No delamination	With delamination
A	200x100	1917	2350
B	200x80	2264	1606
C	200x66	1618	1136

Table 3: Comparison of experimental result with numerical value

Specimen name	No delamination (N)		With delamination (N)	
	Experiment	ANSYS	Experiment	ANSYS
A	1050	1917	1150	2350
B	2150	2264	650	1606
C	1850	1618	1000	1136

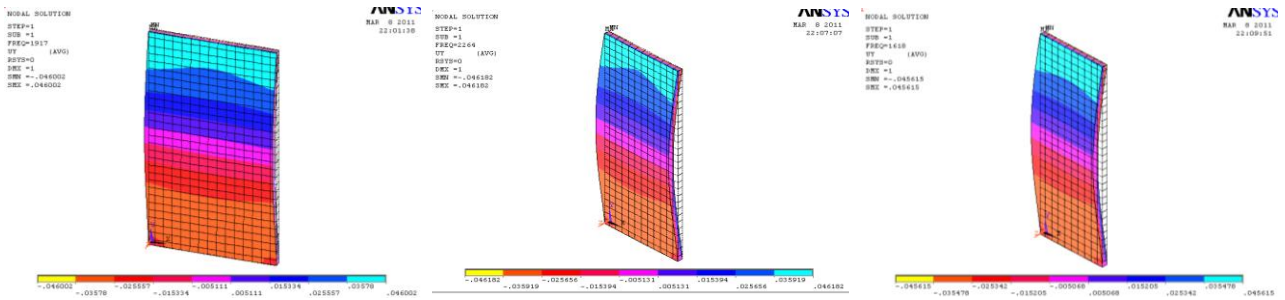

(a) Specimen-A (b) Specimen-B (c) Specimen-C

Fig. 5: Buckling mode shape of specimen without delamination

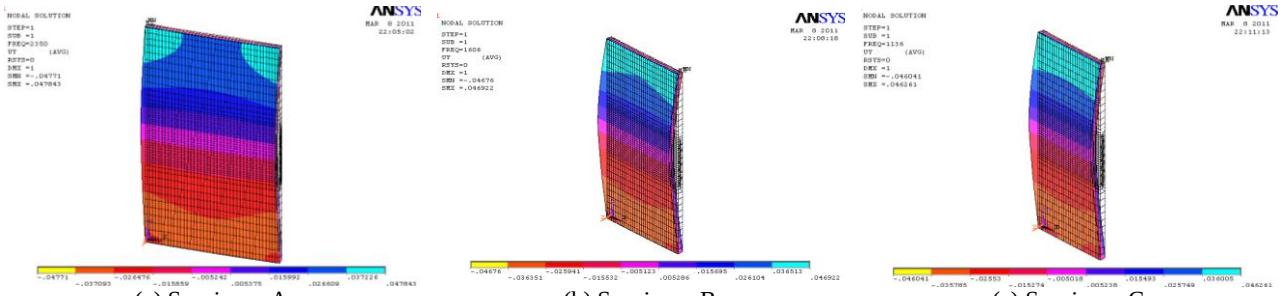

(a) Specimen-A (b) Specimen-B (c) Specimen-C

Fig. 6: Buckling mode shape of specimen with delamination

5. Conclusion

The experimental buckling strength of the composite plate (90°/ 45°/ -45°/ 0°) S has been analysed at it is both the ends simply supported, and the other two edges are free. The buckling strength has been evaluated experimentally by drawing a graph load vs displacement. From the graph, the buckling strength can be found at the intersection of tangents of two deviating curves. In all the specimens, the buckling strength has been reduced with increasing the aspect ratio. This reduction is found to be more efficient when the aspect ratio is read from 2.5 to 3. When the laminates are without delamination and with delamination for the aspect ratio of 2.5 are compared and found that the buckling strength of the without delamination is 2264 N and with delamination is 1606 N, and similarly, it has 29% reduction in buckling strength. Hence delamination of the laminate weakens the resistance to the buckling. The present work could be extended to various types of stacking sequences of the composite laminate, and the analysis can be extended to different end conditions.

REFERENCES:

[1] J.K. Kocsis and T. Bárány. 2014. Single-polymer composites (SPC): status and future trends, *Compos. Sci. Tech.*, 92, 77-94. https://doi.org/10.1016/j.compscitech.2013.12.006.

[2] L. Mészáros and J. Szakács. 2016. Low-cycle fatigue properties of basalt fibre and graphene reinforced polyamide 6 hybrid composites, *J. Reinf. Plast. Compos*, 35(22), 1671-1681. https://doi.org/10.1177/0731684416665176.

[3] T. Shalu and M.A. Joseph. 2009. Development and characterization of liquid CFR aluminium matrix composite, *J. Mater. Process. Tech.*, 209(10), 4809-4813. https://doi.org/10.1016/j.jmatprotec.2008.12.012.

[4] G.J. Simitses and W.L. Yin. 1985. Effect of delamination of axially loaded homogeneous laminated plates, *AIAA J.*, 23(9), 1437-1444. https://doi.org/10.2514/3.9104.

[5] Padmanavdash and B.N. Singh. 2012. Buckling and post-buckling of laminated composite plates, *Mech. Res. Commun.*, 46, 1-7. https://doi.org/10.1016/j.mechrescom.2012.08.002.

[6] J.S. Anastasiadis and G.J. Simitses. 1991. Spring simulated delamination of axially-loaded flat laminates, *Composite Structures*, 17(1), 67-85. https://doi.org/10.1016/0263-8223(91)90061-3.

[7] H.R. Ovesya, M.A.S. Mooneghia and M. Kharazib. 2015. Post-buckling analysis of delaminated composite laminates with multiple through-the-width delaminations using a novel layerwise theory, *Thin-Walled Struct.*, 94, 98-106. https://doi.org/10.1016/j.tws.2015.03.028.

[8] H. Huang and G.A. Kardomateas. 1997. Post-buckling analysis of multiply delaminated composite plates, *J. Appl. Mech.*, 64(4), 842. https://doi.org/10.1115/1.2788990.

[9] G.A. Kardomateas. 1989. Large deformation effects in the post-buckling behaviour of composites with thin delaminations, *AIAA J.*, 27(5), 624-631. https://doi.org/10.2514/3.10153.

[10] H. Ovesy, M. Naghinejad and M. Kharazi. 2016. Delamination growth speed analysis in a compressed composite laminate based on first-order shear deformation theory, *J. Compos. Mater.*, 50(6), 849-857. https://doi.org/10.1177/0021998315583074.

[11] T.H.K. Keith and Kedward. 1999. A method for modelling the local and global buckling of delaminated composite plates, *Compos. Struct.*, 44(1), 43-53. https://doi.org/10.1016/S0263-8223(98)00117-2.

[12] A. Karrech, M. Elchalakani, M. Attar and A.C. Seibi. 2017. Buckling and post-buckling analysis of geometrically non-linear composite plates exhibiting large initial imperfections, *Compos. Struct.*, 174, 134-141. https://doi.org/10.1016/j.compstruct.2017.04.029.

[13] S. Samborski. 2016. Numerical analysis of the DCB test configuration applicability to mechanically coupled fiber reinforced laminated composite beams, *Compos. Struct.*, 152, 477-487. https://doi.org/10.1016/j.compstruct.2016.05.060.

[14] Z. Juhasz and A. Szekrenyes. 2015. Progressive buckling of a simply supported delaminated orthotropic rectangular composite plate, *Int. J. Solids Struct.*, 69-70, 217-229. https://doi.org/10.1016/j.ijsolstr.2015.05.028.

[15] A. Rhead, R. Butler and G. Hunt. 2012. Compressive strength following delamination induced interaction of panel and sub-laminate buckling, *Proc. 53rd AIAA/ASME/AHS/ASC Structures, Structural Dynamics and Materials Conf.*, Honolulu, Hawaii.

[16] O. Namdar and H. Darendeliler. 2017. Buckling, post buckling and progressive failure analyses of composite laminated plates under compressive loading, *Compos. Part B Engg.*, 120, 143-151. https://doi.org/10.1016/j.compositesb.2017.03.066.

[17] X. Xia, J. Yin, B. Su, D. Hui, R. Yu and X. Liu. 2017. Quantitative determining interface information of nanocomposite by synchrotron radiation small-angle X-ray scattering, *Compos. Part B Engg.*, 120, 92-96. https://doi.org/10.1016/j.compositesb.2017.03.058.

[18] H. Chai, C.D. Babcock and W.G. Knauss. 1981. One-dimensional modelling of failure in laminated plates by delamination buckling, *Int. J. Sol. Struct.*, 17(11), 1069-1083. https://doi.org/10.1016/0020-7683(81)90014-7.

[19] S. Liu, T. Yu, T.Q. Bui, S. Yin, D.K. Thai and S. Tanaka. 2017. Analysis of functionally graded plates by a simple locking-free quasi-3D hyperbolic plate isogeometric method, *Compos. Part B Engg.*, 120, 182-196. https://doi.org/10.1016/j.compositesb.2017.03.061.

[20] Y. Bai, T. Liu, P. Cheng, S. Yuan, D. Yao and G. Tang. 2016. Buckling stability of steel strip reinforced thermoplastic pipe subjected to external pressure, *Compos. Struct.*, 152, 528-537. https://doi.org/10.1016/j.compstruct.2016.05.051.

[21] G. Sun, S. Li, Q. Liu, G. Li and Q. Li. 2016. Experimental study on the crashworthiness of empty / aluminium foam / honeycomb - filled CFRP tubes, *Compos. Struct.*, 152, 969-993. https://doi.org/10.1016/j.compstruct.2016.06.019.

[22] K.C. Shin, W.S. Kim and J.J. Lee. 2007. Application of stress intensity to design of anisotropic / isotropic bi-materials with a wedge, *Int. J. Solids Struct.*, 44(24), 7748-7766. https://doi.org/10.1016/j.ijsolstr.2007.05.014.

[23] J.H. Kim and J.J. Vlassak. 2007. Perturbation analysis of an undulating free surface in a multi-layered structure, *Int. J. Solids Structures*, 44(24), 7924-7937. https://doi.org/10.1016/j.ijsolstr.2007.05.025.

[24] B. Kim, J. Choi, S. Yang, S. Yu and M. Cho, 2017 Multiscale modeling of interphase in crosslinked epoxy nanocomposites, *Compos. Part B Engg.*, 120, 128-142. https://doi.org/10.1016/j.compositesb.2017.03.059.

[25] H.R. Ovesy and M. Kharazi, 2011 Compressional stability behaviour of composite plates with through-the-width and embedded delamination by using first-order shear deformation theory, *Comp. Stru.*, 89(19-20), 1829-1839. https://doi.org/10.1016/j.compstruc.2010.10.016.

[26] S. Sivasaravanan and V.K.B. Raja. 2014. Impact characterization of epoxy LY556/E-glass fibre/nano clay hybrid nano composite materials, *Proc. Engg.*, 97, 968-974. https://doi.org/10.1016/j.proeng.2014.12.373.